



Universiteit  
Leiden  
The Netherlands

## Personalized treatment for von Willebrand disease by RNA-targeted therapies

Jong, A. de

### Citation

Jong, A. de. (2020, April 7). *Personalized treatment for von Willebrand disease by RNA-targeted therapies*. Retrieved from <https://hdl.handle.net/1887/136853>

Version: Publisher's Version

License: [Licence agreement concerning inclusion of doctoral thesis in the Institutional Repository of the University of Leiden](#)

Downloaded from: <https://hdl.handle.net/1887/136853>

**Note:** To cite this publication please use the final published version (if applicable).

Cover Page



Universiteit Leiden



The handle <http://hdl.handle.net/1887/136853> holds various files of this Leiden University dissertation.

**Author:** Jong, A. de

**Title:** Personalized treatment for von Willebrand disease by RNA-targeted therapies

**Issue date:** 2020-04-07



# 8

## **Amelioration of the murine von Willebrand disease type 2B phenotype using an allele-specific small interfering RNA**

Annika de Jong  
Caterina Casari  
Richard Dirven  
Bart van Vlijmen  
Peter Lenting  
Cécile Denis  
Jeroen Eikenboom

*In preparation*

## Abstract

Von Willebrand disease (VWD) type 2B is caused by dominant negative mutations in the platelet binding site within von Willebrand factor (VWF), resulting in an increase in VWF that circulates in its 'activated' state (active VWF), spontaneous platelet binding and subsequent thrombocytopenia. Since small interfering RNAs (siRNAs) can distinguish two *VWF* alleles by only one nucleotide, we hypothesized that an siRNA that inhibits production of the dominant negative VWD type 2B mutation VWF p.Val1316Met, but not wild type VWF, could correct the VWD type 2B phenotype. In this study we aim to prove the concept of allele-specific *VWF* inhibition in a heterozygous VWD type 2B mouse model via siRNA-mediated allele-specific inhibition. VWF deficient mice hydrodynamically injected with both wild type and mutant mouse *Vwf* (m*Vwf*) p.Val1316Met cDNA were used. We show that these mice recapitulate the human VWD type 2B phenotype with low platelet counts and an increase in active mVWF. An *in vitro* siRNA screen in HEK293 cells overexpressing m*Vwf* alleles resulted in the selection of an siRNA that selectively inhibited production of the mutant allele with minor inhibition of the wild type allele. Injection of this siRNA in heterozygous VWD type 2B mice resulted in strong VWF downregulation where the siRNA had a higher ability to inhibit the mutant allele over the wild type allele. This resulted in clear improvements in the platelet phenotype. Altogether, we showed that allele-specific siRNAs are capable of correcting a VWD type 2B phenotype in mice. These results are promising for further developments of RNA-targeted therapies for VWD.

## Introduction

Von Willebrand disease (VWD) is the most common inherited bleeding disorder and is in most cases caused by dominant negative mutations in von Willebrand factor (VWF).<sup>1</sup> VWF is a large multimeric glycoprotein that is secreted from endothelial cells upon vascular damage. Once secreted, vascular shear unfolds VWF into ultra large VWF strings that are attached to the exposed collagen.<sup>2</sup> The elongated structure of VWF allows binding of platelets via their glycoprotein Iba receptor to the A1 domain of VWF, starting platelet adhesion and subsequent platelet activation and aggregation at sites of vascular damage.<sup>3</sup>

Several types of VWD can be distinguished due to either qualitative or quantitative defects in VWF. VWD type 2B is one of the qualitative VWD types and is caused by dominant negative gain-of-function mutations in the platelet's glycoprotein Iba binding site in the A1 domain of VWF.<sup>4</sup> These mutations cause a conformational change of the VWF A1 domain and therefore allow platelets to bind VWF without activation of VWF by vascular shear for example.<sup>5,6</sup> Furthermore, the VWF-platelet complexes are cleared rapidly and most VWD type 2B patients present with low platelet counts, either at steady state or in situations of increased VWF release.<sup>7,8</sup>

Mutations at a few locations within the A1 domain of VWF are responsible for VWD type 2B.<sup>4</sup> VWF p.Val1316Met leads to one of the most severe VWD type 2B phenotypes and patients with this mutation present with a very low platelet count, decreased VWF plasma levels and giant platelets.<sup>9</sup> Treatment of VWD type 2B can in some situations be problematic. Desmopressin, which mediates short-term release of VWF from endothelial cells, is generally contra-indicated because increased release of mutant VWF leads to an even further drop in platelet count. VWF-containing concentrates, on the other hand, are able to correct for the bleeding phenotype in most situations.<sup>10</sup> However, pregnancy, surgery or inflammation may lead to stress-induced release of endogenously produced mutant VWF from endothelial cells.<sup>9-12</sup> This may lead to a deep thrombocytopenia which cannot be prevented by administration of an exogenous source of VWF-containing concentrates and may even require platelet transfusion.<sup>13</sup>

We hypothesize that specific inhibition of the production of mutant VWF, without affecting the production of normal VWF, will have a positive effect on VWF function and might be a solution for VWD patients with an unmet clinical need, such as the VWD type 2B patients described above.<sup>14,15</sup> We previously showed that allele-specific siRNAs that target frequent single-nucleotide polymorphisms within *VWF* are able to distinguish two *VWF* alleles based on one nucleotide variation.<sup>14</sup> Targeting a heterozygous SNP located on the same allele as the dominant negative mutation has already proven successful *in vitro* (HEK293 cells<sup>14</sup>) and *ex vivo* (endothelial colony forming cells<sup>16</sup>). Here, we extend this proof of concept of allele-specific *VWF* inhibition to a mouse model of heterozygous VWD type 2B. Since in-bred mice do not contain (human) heterozygous variations, we cannot discriminate between *VWF* alleles

with the SNP-targeted approach in mice. Therefore, instead of targeting a heterozygous SNP linked to the dominant negative mutation, we have designed siRNAs that target the dominant negative mouse VWD type 2B mutation, p.Val1316Met, itself. Heterozygous VWD type 2B mice were generated by hydrodynamic injection of both wild type mouse *Vwf* (m*Vwf*) and mutant m*Vwf* p.Val1316Met cDNA in VWF deficient ( $^{-/-}$ ) mice. Injection of an siRNA that targets the m*Vwf* p.Val1316Met cDNA sequence in heterozygous VWD type 2B mice resulted in strong inhibition of the mutant allele and correction of the VWD type 2B platelet phenotype.

## Methods

### **Plasmid expression vectors**

Full length mouse *Vwf* (m*Vwf*) cDNA was obtained by NotI and XbaI restriction of pLIVE®-m*Vwf*.<sup>17</sup> Both restriction sites were introduced in the pLIVE® plasmid by the Q5® Site-Directed Mutagenesis Kit (New England Biolabs, Ipswich, MA, USA). The obtained m*Vwf* cDNA was ligated into pcDNA™3.1/Zeo (+) using the DNA Ligation Kit for Long Fragments (Takara, Saint-Germain-en-Laye, France). The mVWF p.Val1316Met mutation (c.3946G>A) was introduced in pcDNA™3.1/Zeo (+) m*Vwf* by the Q5® Site-Directed Mutagenesis Kit to obtain pcDNA™3.1/Zeo (+) m*Vwf*-p.Val1316Met. A Myc peptide tag was introduced at the C-terminal end of mVWF to create pcDNA™3.1/Zeo (+) m*Vwf*/Myc and was used to distinguish wild type mVWF from mVWF-p.Val1316Met on a protein level *in vitro*. For *in vivo* experiments, we ligated m*Vwf*/Myc and m*Vwf*-p.Val1316Met back into pLIVE®, and introduced an HA tag at the C-terminal end of m*Vwf*-p.Val1316Met to create m*Vwf*-p.Val1316Met/HA. Plasmids for *in vivo* application were purified using NucleoBond® PC 2000 EF (Macherey-Nagel, Düren, Germany).

### **siRNA design**

Four custom Silencer® Select 21-mer siRNA oligonucleotides (Ambion, Life Technologies Europe BV) with a dTdT overhang at the 5' end of the sense strand were designed to fully complement the m*Vwf* p.Val1316Met mutation (c.3946A) and therefore have one mismatch with the wild type allele (c.3946G). To create more specific siRNAs (i.e. decreased potency for the untargeted allele), nine siRNAs were designed that contain one extra mismatch next to the mutation. siRNA sequences are summarized in Fig. 1A. For *in vitro* siRNA screening, we used custom synthesized Silencer Select siRNAs with standard purification (Thermo Fisher Scientific, Carlsbad, CA, USA: 4390827) and Ambion® Silencer® Select Negative Control siRNA (Thermo Fisher Scientific: 4404020) as negative control (siNEG). For *in vivo* experiments, we used custom synthesized Silencer Select siRNAs with HPLC purification (Thermo Fisher Scientific: 4390831).

### **Cell culture and transfection**

siRNA and plasmid transfections in Human Embryonic Kidney 293 (HEK293) cells (ATCC, Rockville, MD, USA) were performed as described before.<sup>14</sup> Screening of the designed siRNAs for efficiency and specificity was performed by cotransfection of mVwf/Myc or mVwf-p.Val1316Met plasmid with 2 nM siRNA in separate wells. *In vitro* improvements in the function of mVWF was investigated in HEK293 cells cotransfected with mVwf/Myc, mVwf-p.Val1316Met and siRNA in the same well. mVwf plasmids were always transfected in a total plasmid concentration of 600 ng/mL.

### **Mouse experiments**

Hydrodynamic gene transfer of mVwf plasmids was performed in 8-12 weeks old male/female VWF<sup>-/-</sup> mice on a C57BL/6 background as described before.<sup>17</sup> In short, a total amount of 40 or 50 µg plasmid (indicated per experiment) was diluted in 0.9% sodium chloride in a volume that is equivalent to 10% of the body weight. Diluted plasmid was injected through the tail vein in approximately 5 seconds. To generate heterozygous VWD type 2B mice, equal quantities of pLIVE<sup>®</sup> mVwf/Myc and pLIVE<sup>®</sup> mVwf-p.Val1316Met/HA were injected. Five days after plasmid injections, siRNAs in a final concentration of 0.5 or 1 mg/kg were injected through the tail vein and directed to the liver by the use of InvivoFectamine 3.0 Reagent (Thermo Fisher Scientific) following the manufacturer's instructions. At indicated time points, blood was drawn in 10% EDTA (final concentration: 50 mM) or citrate (final concentration: 13.8 mM) from the retro-orbital plexus under isoflurane anesthesia. All animal experiments were performed with approval of the local ethical committee CEEA26 under the number APAFIS#20037-2019032714308918 v3.

### **Blood analysis**

Platelet count and platelet volume were determined in whole EDTA blood using a veterinary cell counter (Scil Vet ABC Plus, Horiba Medical, France), except for one experiment in which flow cytometry was used. For flow cytometry analysis, whole blood was diluted 20 times in phosphate-buffered saline (PBS). Platelets in diluted blood were stained for 15 minutes with a FITC labeled rat anti-mouse CD41 antibody (cat: 553848, BD Pharmingen, San Jose, CA, USA) at room temperature. Samples were directly analyzed with an Accuri C6 flow cytometer (BD Biosciences, Le Pont de Claix, France).

### **Staining of blood smears and liver sections**

Blood smears were prepared from EDTA blood and stained using Kwik-DIFF (Thermo Fisher Scientific) and imaged using the 3DHistech Panoramic 250 slide scanner.

Whole livers were embedded in Tissue-Tek O.C.T. (Sakura, Alphen aan den Rijn, The Netherlands) and snap frozen. 5  $\mu\text{m}$  cryosections were fixed by ethanol containing 5% acetic acid (ice-cold) and blocked with PBS supplemented with 10% normal goat serum (Dako, Glostrup, Denmark). Rabbit anti-HA (Cell signaling, Leiden, the Netherlands), rat anti-Myc (Chromotek, Martinsried, Germany) or isotype controls were diluted in blocking buffer and liver sections were incubated with primary antibodies for 45 minutes. Liver sections were incubated with secondary antibodies goat anti-rat IgG (H+L) AF488 and goat anti-rabbit IgG (H+L) AF594 (Thermo Fisher Scientific) diluted in blocking buffer for 30 minutes. Stained sections were mounted using ProLong Gold (Life Technologies) and imaged using the 3DHistech Panoramic 250 slide scanner.

### ***VWF quantification and functional assays***

Total mVWF, mVWF/Myc and mVWF/HA protein levels were measured in plasma, and total mVWF and mVWF/Myc protein levels were measured in conditioned medium as described before<sup>14</sup> with the modification that sheep anti-VWF (ab11713; Abcam, Cambridge, United Kingdom) was used as coating antibody for the mVWF/HA ELISA. A pool of normal mouse plasma (NMP) from wild type C57BL/6J mice was used as a reference for the mVWF:Ag ELISA. NMP was prepared the same as the plasma samples of individual mice. Recombinant mVWF/Myc and mVWF/HA produced by HEK293 cells was used as reference in the mVWF/Myc and mVWF/HA ELISA and normalized to mVWF:Ag levels measured in NMP. All antigen data is represented as percentage of NMP.

Active mVWF was measured using the AU/VWFA-11 nanobody that captures only mVWF in which the A1 domain is in its open conformation.<sup>5</sup> This nanobody was a kind gift of Dr. Rolf Urbanus (Utrecht Medical Center, Utrecht, the Netherlands). ELISA plates were coated with the AU/VWFA-11 nanobody diluted in coating buffer (100 mM bicarbonate, 500 mM sodium chloride, pH 9.0) overnight at 4°C. Wells were blocked thereafter with PBS containing 3% bovine serum albumin (BSA; Sigma-Aldrich, St Louis, MO, USA) for 30 minutes at 37°C. Samples (conditioned medium or plasma) were diluted in PBS containing 3% BSA in 3 mVWF:Ag concentrations (5.0, 3.4 and 1.7 percent of NMP) and incubated for 2 hours at 37°C. To increase the signal in the ELISA, we conjugated biotin (Sigma-Aldrich) to rabbit anti-VWF-IgG (A0082; Dako) to create rabbit anti-VWF-IgG-biotin. Wells were incubated with rabbit anti-VWF-IgG-biotin diluted in PBS containing 3% BSA for 1 hour at 37°C. Streptavidin-(POLY) horseradish peroxidase (Thermo Fisher Scientific) in PBS containing 3% BSA was used as detecting antibody and wells were incubated with detecting antibody for 1 hour at 37°C. Wells were incubated with 1 tablet of O-phenylenediamine dihydrochloride (Sigma-Aldrich) dissolved in 11 ml substrate buffer (22 mM citric acid, 51 mM phosphate, pH 5.0) and 11  $\mu\text{l}$  30%  $\text{H}_2\text{O}_2$ . The enzymatic reaction was stopped using 2M  $\text{H}_2\text{SO}_4$ . Slopes were calculated per sample from the extinctions obtained



from the three dilutions that were plated per sample. The mVWF activation factor of a plasma sample was calculated by dividing the slope of a plasma sample over the average of the slopes of plasma from mice injected with (wild type) mVwf/Myc cDNA only. The mVWF activation factor of conditioned medium samples was calculated by dividing the slope of a conditioned medium sample over the average of the slopes of conditioned media from cells transfected with wild type mVwf/Myc only.

### **Statistical analysis**

Graphic illustrations were generated using GraphPad Prism 8.0.1 (GraphPad Software, La Jolla, CA, USA). The Mann-Whitney *U* or Kruskal-Wallis test was used to investigate significance between two or three groups, respectively. Wilcoxon matched-pairs signed rank test or Friedman test was used to assess significance between before and after siRNA treatment. *P* < 0.05 was considered statistically significant. All data is represented as the median with the range, unless otherwise stated.

## **Results**

### ***In vitro* selection of efficient and allele-specific siRNAs**

Four siRNAs were designed to be fully complementary with mutant mVwf p.Val1316Met, and therefore had one mismatch with the wild type allele (Fig. 1A). Cotransfection of these siRNAs with either wild type mVwf/Myc or mutant mVwf-p.Val1316Met plasmids in HEK293 cells revealed that siRNA-1 efficiently inhibited total mVWF, but was not specific to the mutant allele. siRNA-2, -3 and -4 on the other hand were neither efficient nor very specific (Fig. 1B). It was previously shown that addition of one extra mismatch in an allele-specific siRNA might improve the specificity of the siRNA.<sup>18-20</sup> We therefore designed nine variations on siRNA-1 with additional mismatches at different positions of the siRNA (Fig. 1A) and transfected these siRNAs with either mVwf/Myc or mVwf-p.Val1316Met plasmids. Two of the newly designed siRNAs (siRNA-1-14G and siRNA-1-10U) were clearly more specific for the mutant allele, while retaining efficiency (Fig. 1B). These two siRNAs were selected for further experiments.

Cotransfections of mVwf/Myc and mVwf-p.Val1316Met plasmids with either siRNA-1-14G or siRNA-1-10U were performed to investigate whether competition between both alleles increases the specificity of the siRNAs and to observe whether the siRNAs could correct for a VWD type 2B phenotype *in vitro*. Clear inhibition of mutant mVWF-p.Val1316Met was already observed for both siRNAs at an siRNA concentration of 0.5 nM with no inhibition of wild type mVWF/Myc. Also at higher siRNA concentrations, we observed minor inhibition of mVWF/Myc, especially for siRNA-1-10U (Fig. 1C and 1D). Improvements in the VWD type 2B phenotype

were assessed in conditioned medium using the active mVWF ELISA that detects the open conformation of the mVWF A1 domain. Compared to siNEG treated cells, both siRNA-1-14G and siRNA-1-10U treated cells showed a decrease in the presence of dysfunctional mVWF by a decrease in the mVWF activation factor. siRNA-1-10U was superior over siRNA-1-14G. We therefore chose siRNA-1-10U as our lead compound for the *in vivo* experiments.

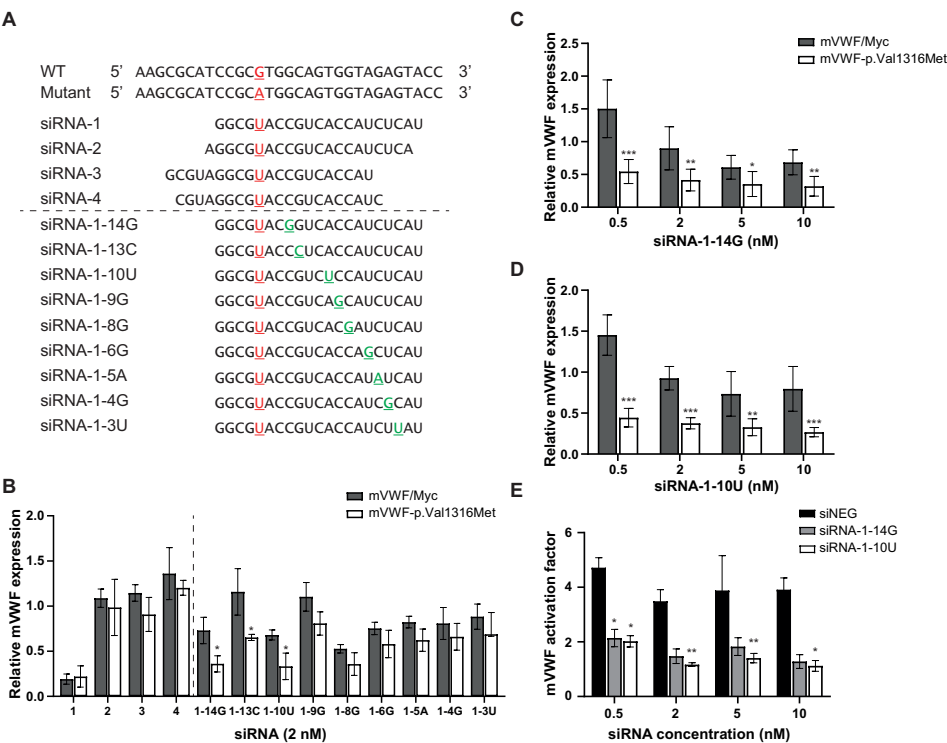


**Figure 1. *In vitro* siRNA screen in HEK293 cells.** (A) mRNA sequences of the wild type (WT) and mutant allele surrounding the nucleotide responsible for the p.Val1316Met mutation and the sequences of the antisense strand of siRNAs designed to target the p.Val1316Met mutation in mice. The red nucleotide in the siRNAs indicates the nucleotide that is complementary to the mutant allele, but is mismatched with the wild type allele. The green nucleotides indicate an extra mismatch that was incorporated in siRNA-1 to make the siRNA more specific to inhibit the mutant allele only. (B) siRNA screen in HEK293 cells. Bars represent mVWF levels measured in conditioned medium of HEK293 cells cotransfected with either mVwf/Myc or mVwf-p.Val1316Met plasmids and 2 nM siRNA, normalized to mVWF levels measured in conditioned medium of HEK293 cells cotransfected with either mVwf/Myc or mVwf-p.Val1316Met and a negative control siRNA (siNEG). Shown are the mean  $\pm$  1 SD of two independent experiments performed in duplicate, except for siRNA-1 that was tested three times in duplicate. Mann-Whitney, \*  $P < 0.05$  (C, D) Normalized mVWF/Myc and mVWF-p.Val1316Met protein levels measured in conditioned medium of HEK293 cells cotransfected with mVwf/Myc, mVwf-p.Val1316Met and (C) siRNA-1-14G or (D) siRNA-1-10U. siRNAs were transfected at concentrations of 0.5, 2, 5 and 10 nM and protein levels were normalized to the mVWF/Myc and mVWF-p.Val1316Met protein levels measured in conditioned medium of HEK293 cells cotransfected with mVwf/Myc, mVwf-p.Val1316Met and siNEG. Shown are the mean  $\pm$  1 SD of four independent experiments performed in duplicate. Mann-Whitney, \*  $P < 0.05$ , \*\*  $P < 0.01$ , \*\*\*  $P < 0.001$  (E) The mVWF activation factor measured in conditioned medium of HEK293 cells cotransfected with mVwf/Myc, mVwf-p.Val1316Met and siRNA-1-14G, siRNA-1-10U or siNEG. Shown are the mean  $\pm$  1 SD of two independent experiments performed in duplicate. Kruskal-Wallis, \*  $P < 0.05$ , \*\*  $P < 0.01$ . HEK293, Human Embryonic Kidney 293; mVWF, mouse von Willebrand factor; nM, nanomolar; siRNA, small interfering RNA; WT, wild type

### Generation of a heterozygous mouse model for VWD type 2B

Hydrodynamic gene transfer of mutant *mVwf* cDNA in *VWF<sup>-/-</sup>* mice has frequently been used to study phenotypic effects of known VWD mutations.<sup>17,21</sup> Most of these studies inject solely mutant *mVwf* cDNA, however in our approach of allele-specific inhibition of mutant *mVwf* we require a heterozygous model.<sup>22</sup> A heterozygous VWD type 2B mouse model was therefore generated by hydrodynamic injection of equal amounts of both *mVwf/Myc* and *mVwf-p.Val1316Met/HA* cDNA in *VWF<sup>-/-</sup>* mice. Four days after hydrodynamic injection, we observed equal expression of both products in plasma for all mice (Fig. 2A). This resulted in a deep drop in platelet count in five out of six mice as compared to mice expressing *mVWF/Myc* only ( $P = 0.052$ , Fig. 2B). No decreased platelet count was observed in one mouse, however, the total *mVWF:Ag* levels in this mouse were relative low (111%), which might have been insufficient to induce the VWD type 2B platelet phenotype. Furthermore, injection of both *mVwf/Myc* and *mVwf-p.Val1316Met/HA* cDNA in *VWF<sup>-/-</sup>* mice resulted in a significant increase in dysfunctional *mVWF* as represented by the increased *mVWF* activation factor, compared to *VWF<sup>-/-</sup>* mice injected with *mVwf/Myc* cDNA only ( $P < 0.01$ , Fig. 2C). This increase in the *mVWF* activation factor was also observed for the mouse without a decreased platelet count. The VWD type 2B platelet phenotype was confirmed by analysis of blood smears from the heterozygous VWD type 2B mice. These smears contained only small numbers of platelets, which were usually observed in aggregates (Fig. 2D). Liver sections were stained for *mVWF/Myc* and *mVWF-p.Val1316Met/HA* using anti-Myc and anti-HA antibodies to investigate the distribution of both gene products in the liver. Interestingly, the hepatocytes that internalized plasmid, always internalized both plasmids as represented by the colocalization of anti-Myc and anti-HA staining (Fig. 2E). Altogether, this indicates that the model used represents a true heterozygous mouse model for VWD.

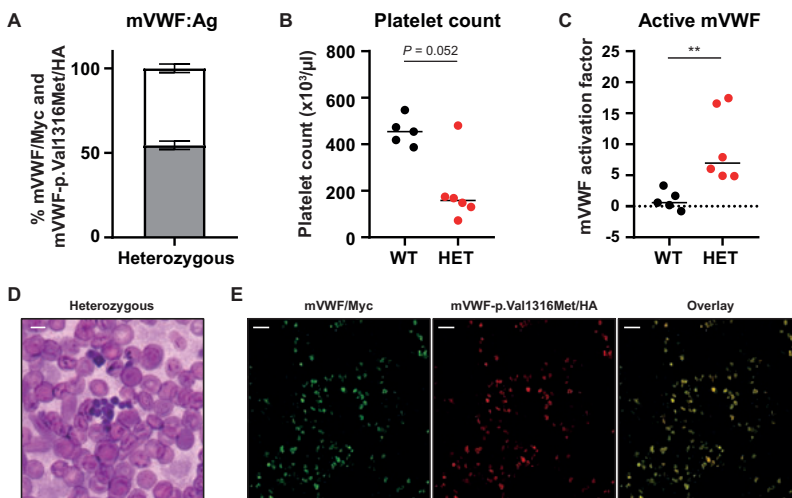


**Figure 2. Characteristics of heterozygous VWD type 2B mice.** (A) Distribution of *mVWF/Myc* (white bar) and

mVWF-p.Val1316Met/HA (grey bar) in plasma of VWF<sup>-/-</sup> mice four days after injection of equal quantities (25 µg) of both plasmids. Expression of both plasmids is approximately equal. (B) Platelet count and (C) mVWF activation factor of VWF<sup>-/-</sup> mice, four days after injection of mVwf/Myc (WT) cDNA only or co-injection of mVwf-p.Val1316Met/HA and mVwf/Myc (HET) cDNA. The horizontal lines in the graphs show the median and the dots represent single mice. Mann-Whitney, \*\*  $P < 0.01$  (D) Representative blood smear of a heterozygous VWD type 2B mouse, four days after injection of both mVwf/Myc and mVwf-p.Val1316Met/HA cDNA in VWF<sup>-/-</sup> mice. Platelet aggregates are observed. Bar represents 5 µm. (E) Staining of mVWF/Myc and mVWF-p.Val1316Met/HA in liver sections (5 µm thickness) generated from livers harvested from VWF<sup>-/-</sup> mice, four days after injection of both mVwf/Myc and mVwf-p.Val1316Met/HA. Stainings were performed using antibodies directed to Myc (green) and HA (red). Clear co-expression of both alleles is observed in all hepatocytes that express mVWF (colocalization in yellow). No hepatocytes are observed with mVWF/Myc or mVWF-p.Val1316Met/HA only. Bar represents 100 µm. HET, heterozygous; mVWF, mouse von Willebrand factor; WT, wild type

### ***In vivo correction of the VWD type 2B phenotype***

The heterozygous VWD type 2B mice showed a clear phenotype, four days after hydrodynamic injection of both mVwf/Myc and mVwf-p.Val1316Met/HA cDNA. To investigate whether the *in vitro* selected siRNA against mVwf p.Val1316Met (siRNA-1-10U) could correct the *in vivo* type 2B phenotype, we injected siRNA-1-10U in a concentration of 1 mg/kg, five days after hydrodynamic injection (N = 6). Two days after injection of siRNA-1-10U, a strong 88% knockdown of total mVWF was observed with a relative specificity of siRNA-1-10U towards the mutant allele (Table 1). Of note, also untreated heterozygous VWD type 2B mice showed on average 44% reduced mVWF:Ag levels at this day (Table 1). Specificity of siRNA-1-10U to inhibit the mutant allele is clearly indicated by the percentage of mVWF-p.Val1316Met/HA in plasma that decreased from 57% (55%-58%) to 32% (25%-42%) of total plasma mVWF ( $P < 0.05$ ; Fig. 3A). This coincided with a strong increase in platelet count ( $P = 0.063$ ; Fig. 3B). Platelet count was not increased for one mouse after siRNA-1-10U treatment. Another mouse did not show a decrease in platelet count after hydrodynamic injection, precluding the possibility of correction. Platelet size is known to be increased in mice injected with mVwf-p.Val1316Met cDNA.<sup>17,23</sup> The forward scatter in flow cytometry measurements could be used as an estimation of the platelet size. Previous work showed a platelet forward scatter of  $1.3 \times 10^5$  for VWF<sup>-/-</sup> mice injected with wild type mVwf cDNA.<sup>23</sup> In this study, heterozygous VWD type 2B mice showed a platelet forward scatter of  $4.1 \times 10^5$ . Injection of siRNA-1-10U did, however, not result in a decrease of the platelet forward scatter (Fig. 3C). The mVWF activation factor was decreased 1.6 fold after siRNA-1-10U injection, indicating a decrease of the presence of mutant constitutively active mVWF (N = 4; Fig. 3D). mVWF:Ag levels after siRNA injection were too low for two mice to determine the mVWF activation factor. One of these two mice was the mouse with a normal starting platelet count. The other mouse had a low starting platelet count that was increased after siRNA injection. Interestingly, the mouse without correction of the platelet count, did show amelioration in active mVWF with a 1.6 fold decrease in the mVWF activation factor.

**Table 1.** total mVWF, mVWF/Myc and mVWF-p.Val1316Met/HA antigen levels measured in plasma from VWF<sup>-/-</sup> mice hydrodynamically injected with mVwf/Myc and mVwf-p.Val1316Met/HA cDNA

siRNA	Concentration	Sex	Total mVWF (Myc+HA) (% of NMP)				mVWF/Myc (% of NMP)				mVWF-p.Val1316Met/HA (% of NMP)			
			Day -1	Day +2	Day +4	Day +7	Day -1	Day +2	Day +4	Day +7	Day -1	Day +2	Day +4	Day +7
siRNA-1-10U	1 mg/kg	M	1270	196			568	146			702	50		
siRNA-1-10U	1 mg/kg	F	472	22			198	13			274	9		
siRNA-1-10U	1 mg/kg	F	599	42			257	31			342	12		
siRNA-1-10U	1 mg/kg	F	2908	205			1230	140			1677	66		
siRNA-1-10U	1 mg/kg	F	1915	566			864	329			1051	238		
siRNA-1-10U	1 mg/kg	F	1364	151			577	101			787	50		
-	-	M	1284	1497			529	681			755	816		
-	-	M	253	136			101	61			153	75		
-	-	M	415	171			188	81			227	90		
-	-	F	1524	393			737	181			788	213		
-	-	F	2270	1422			1042	628			1228	795		
siRNA-1-10U	0.5 mg/kg	M	4091	830	418	336	1870	525	318	227	2220	305	100	109
siRNA-1-10U	0.5 mg/kg	M	2753	473	257	35	1333	369	209	28	1420	104	48	8
siRNA-1-10U	0.5 mg/kg	M	2888	449	307	401	1455	341	245	301	1433	109	61	100
siRNA-1-10U	0.5 mg/kg	M	1025	114	60	104	573	88	52	89	453	26	7	16
siRNA-1-10U	0.5 mg/kg	F	2849	256	132	209	1422	197	105	166	1427	59	27	43
-	-	M	4675	3263	3274	1151	2172	1539	1612	540	2503	1724	1663	610
-	-	F	380	78	77	90	192	45	40	43	188	33	36	47

F, female; M, male; mg/kg, milligram per kilogram; mVWF, mouse von Willebrand factor; NMP, normal mouse plasma; siRNA, small interfering RNA

Injections of 1 mg/kg siRNA-1-10U resulted in a deep knockdown of total mVWF and most mice had a mVWF expression of less than 200%, two days after siRNA-1-10U injection. It is therefore questionable whether the increase in platelet count after siRNA-1-10U injection was the result of decreased presence of mutant mVWF or that the total levels of mVWF were so low after siRNA-1-10U injection that the level of mutant type 2B VWF was too low to induce the VWD type 2B platelet phenotype. Therefore, we performed a second independent experiment where we injected heterozygous VWD type 2B mice with a lower dose of siRNA-1-10U (0.5 mg/kg; N = 5). A lower siRNA dose may not only lead to reduced inhibition of total mVWF, but potentially also improve specificity for the mutant allele. In this experiment, mice were followed for seven days after siRNA injection to assess the duration of siRNA-1-10U efficacy. Injection of 0.5 mg/kg siRNA-1-10U again led to a clear decrease in total mVWF plasma levels two days after siRNA injection, but the total mVWF:Ag levels were slightly higher (449%) than the total mVWF:Ag levels after injections of 1 mg/kg siRNA-1-10U (197%; Table 1). The percentage of mutant mVWF in plasma of the heterozygous VWD type 2B mice, one day before siRNA-1-10U injection was 50% (44%-54%). This decreased to 23% (22%-37%), 20% (12%-24%) and 21% (15%-33%),

two, four and seven days after siRNA-1-10U injection, respectively (Fig. 3E). Like with the 1 mg/kg dose, platelet counts increased two days after siRNA-1-10U injection (Fig. 3F). Remarkably, a further increase in platelet count was noted four and seven days after siRNA-1-10U injection ( $P < 0.01$ ; Fig. 3F). Also, as was observed after injection of 1 mg/kg siRNA-1-10U, we did not observe a decrease in platelet size two days after 0.5 mg/kg siRNA-1-10U injection. But a statistically significant decrease in platelet size was observed seven days after siRNA-1-10U injection ( $P < 0.01$ ; Fig. 3G). These beneficial effects in platelet phenotype coincided with a strong decrease in active VWF as represented by the decrease in the mVWF activation factor ( $P < 0.01$ ; Fig. 3H). Altogether, comparable results were obtained with siRNA doses of 1 and 0.5 mg/kg and these data indicate that allele-specific siRNAs can improve the VWD type 2B phenotype in mice.

## Discussion

Previously we have shown that allele-specific siRNAs are able to inhibit the production of mutant VWF with minor inhibition of wild type VWF *in vitro* and *ex vivo*.<sup>14-16</sup> In this study, we extended the proof of concept of allele-specific VWF inhibition to a heterozygous VWD type 2B mouse model. Heterozygous VWD type 2B mice were generated by hydrodynamic injection of both wild type and mutant mVwf cDNA (mVwf/Myc and mVwf-p.Val1316Met/HA). These mice phenotypically resemble human VWD type 2B with low platelet counts, increased platelet size and an increase in active mVWF. Clear phenotypic improvements were observed after injection of an siRNA that reduced the production of mVWF-p.Val1316Met/HA but had less affinity to inhibit the production of wild type mVWF/Myc.

As a model for the proof of principle of allele-specific inhibition of mutant mVWF *in vivo* we used VWF<sup>-/-</sup> mice hydrodynamically injected with mutant and wild type mVwf cDNA. Hydrodynamic gene transfer of mVwf cDNA results in hepatic VWF expression while VWF normally is produced in the endothelium and platelets.<sup>17,21</sup> Albeit artificial, hepatic VWF expression has the advantage that it can easily be targeted by siRNAs using InvivoFectamine, a commercially available liposomal formula suited for hepatic siRNA delivery.<sup>24</sup> The proof of concept of allele-specific inhibition in an *in vivo* setting can therefore easily be assessed. Drawback of the model is that hydrodynamic injection may result in supraphysiologic mVWF plasma levels and a wide range in expression levels (Table 1). This, however, did not seem to affect the siRNA efficacy, since the percentage of mutant mVWF after siRNA injection was comparable for all mice, irrespective of starting plasma mVWF levels (Fig. 3A, 3E).

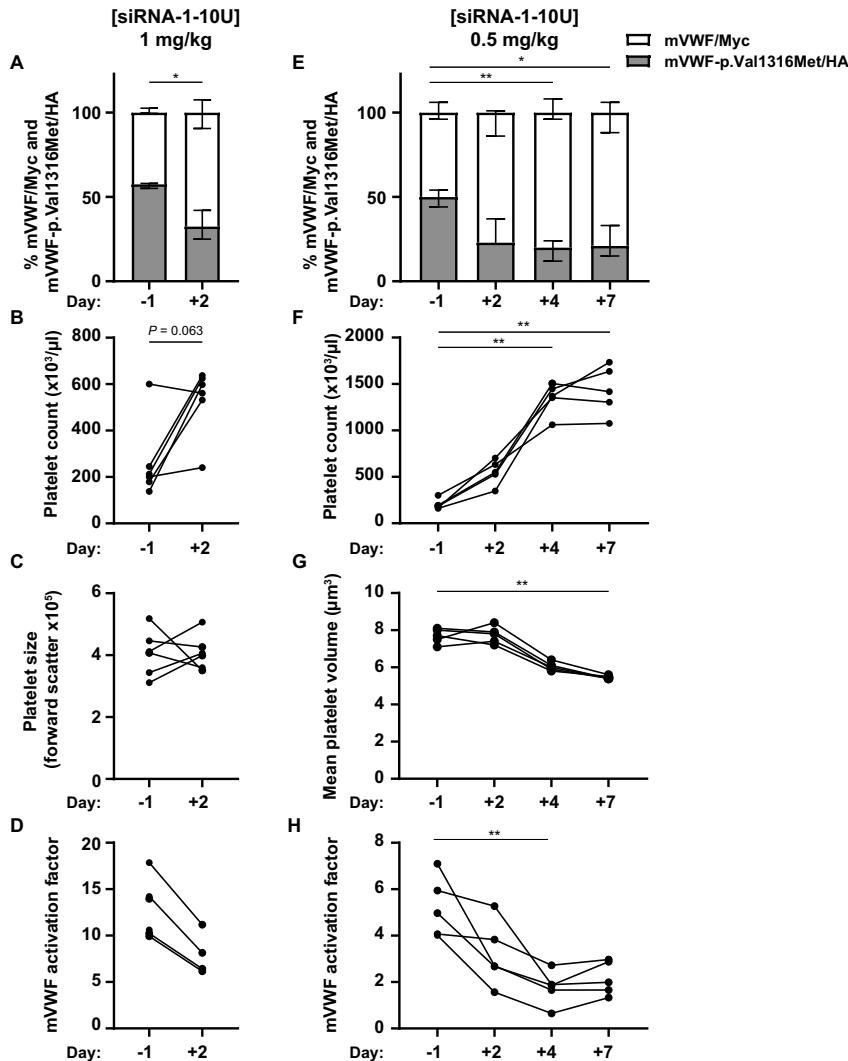


**Figure 3. Correction of the VWD type 2B phenotype.** (A-D) Phenotype improvement of heterozygous VWD type 2B mice injected with 1 mg/kg siRNA-1-10U. (A) Percentage of wild type mVWF/Myc (white bars) and mutant mVWF-p.Val1316Met/HA (grey bars) one day before and two days after siRNA-1-10U injection. Wilcoxon test, \*  $P < 0.05$ . (B) Platelet count measured in mice one day before and two days after siRNA-1-10U injection increased for four out of six mice. One mouse did not respond to siRNA treatment and one mouse had a high starting platelet count, which maintained constant. Wilcoxon test,  $P = 0.063$ . (C) Platelet size, estimated by the forward scatter determined by flow cytometry analysis, was unchanged two days after siRNA-1-10U treatment. (D) A decrease in the mVWF activation factor was observed two days after siRNA-1-10U treatment for four out of six mice. Two mice had too low total mVWF plasma levels to determine the mVWF activation factor. (E-H) Phenotype improvement of heterozygous VWD type 2B mice injected with 0.5 mg/kg siRNA-1-10U. (E) Percentage of wild type mVWF/Myc (white bars) and mutant mVWF-p.Val1316Met/HA (grey bars) one day before and two, four and seven days after siRNA-1-10U injection. Friedman test, \*  $P < 0.05$ , \*\*  $P < 0.01$ . (F) Platelet count increased for all mice after injection of siRNA-1-10U. Friedman test, \*\*  $P < 0.01$ . (G) Platelet size, determined by the veterinary cell counter, was not decreased two days after siRNA injection compared to one day before siRNA injection. Decreased platelet size was observed four and seven days after siRNA-1-10U injection. Friedman test, \*\*  $P < 0.01$ . (H) The mVWF activation factor decreased after siRNA-1-10U injection. Friedman test, \*\*  $P < 0.01$ . mg/kg, milligram per kilogram; mVWF, mouse von Willebrand factor; siRNA, small interfering RNA

Two independent experiments were performed in which siRNAs were injected in heterozygous VWD type 2B mice. With these experiments we aimed to investigate the siRNA concentration needed for allele-specific *mVwf* inhibition in our heterozygous mouse model. In a first experiment, mice were injected with 1 mg/kg siRNA-1-10U. This resulted in rather low total mVWF plasma levels, two days after siRNA injection. Although the plasma levels were rather low, all siRNA-injected mice showed improvements in the ratio of wild type over mutant mVWF and the mVWF activation factor. Furthermore, also platelet count was clearly increased for four out of six mice. It is, however, not possible to confirm that the increase in platelet count was the result of low levels of mutant mVWF or low levels of total mVWF. Especially since a heterozygous VWD type 2B mouse with low total mVWF levels (111%) showed a comparable platelet count to mice injected with wild type *mVwf* cDNA exclusively (Fig. 2B). Even though successful hydrodynamic injection was confirmed in this mouse by expression of both wild type mVWF (43%) and mutant mVWF-p.Val1316Met/HA (57%) and a 4.9 fold increase in the mVWF activation factor.

In a second experiment, we lowered the siRNA dose to 0.5 mg/kg to induce a less strong inhibition of mVWF. Decreasing the siRNA concentration might also lead to better discrepancy between wild type and mutant mVWF, since it is reasoned that a decreased siRNA concentration will first reduce binding of the siRNA to the untargeted allele. Although the sample size is too low to draw definite conclusions, the lower siRNA dose seemed to induce a slightly less strong inhibition of total mVWF and a slight increase in the ratio of wild type mVWF over mutant mVWF-p.Val1316Met compared to mice injected with 1 mg/kg siRNA (Table 1). We also reproduced the increase in platelet count with 0.5 mg/kg siRNA-1-10U. The increase in platelet count is observed in mice with total mVWF:Ag levels above 300%, which is sufficient to induce low platelet counts in *VWF<sup>-/-</sup>* mice injected with mutant *mVwf*-p.Val1316Met cDNA only. However, we have no evidence yet which VWF concentration is sufficient to induce low platelet counts in our heterozygous VWD type 2B mouse model and whether the increase in platelet count after injection of 0.5 mg/kg is indeed caused by a decrease in mutant mVWF and not by a decrease in total mVWF.

Interestingly, a striking increase in platelet count was observed four and seven days after siRNA-1-10U injection, which coincided with normal platelet size values. Platelet counts were even higher than generally is observed in mice hydrodynamically injected with wild type *mVwf* cDNA only.<sup>17,21</sup> This interesting result suggests that there is an increased platelet production, and that these platelets are not cleared through VWF-platelet complexes when there is less mutant VWF present. Besides the increase in platelet count, also a significant decrease in platelet size was observed four and seven days after siRNA injection. This was not observed two days after siRNA injection, which could be explained by the life-time of platelets in mice, which is about four to five days.<sup>25</sup> It might therefore be possible that the persistent increased



platelet size observed two days after siRNA injection, is representative of the large platelets that were still circulating from before the siRNA injection.

A limitation of this study is that we did not include a negative control siRNA in the mouse experiments. Inclusion of a negative control siRNA, preferably a mismatch control, is recommended to prove that the phenotypic improvements are caused by direct effects of the siRNA and to exclude possible off-target effects.<sup>26,27</sup> It is however unlikely that the phenotypic improvements in VWF itself, i.e. decreased mVWF activation factor, are due to an siRNA off-target effect. Also, the allele-specific knockdown effects are unlikely due to off-target effects. However, future studies with a mismatch negative control siRNA should prove that the correction of platelet count and size is indeed the effect of the allele-specific siRNA.

Although siRNA-1-10U has a higher affinity for mutant mVWF, we also observed downregulation of wild type mVWF/Myc *in vitro* and *in vivo*. The most ideal allele-specific siRNA should, however, not be able to inhibit wild type mVWF, even at a high siRNA concentration. Different chemical modification of the siRNA might improve siRNA specificity. In this study, siRNAs with the Locked Nucleic Acid (LNA) modifications were used. LNA is known to stabilize the siRNA and therefore makes the siRNA more potent to its target.<sup>28</sup> Different modifications, like 2' fluoro or 2' O-methyl ribose modifications, might further improve specificity.<sup>29</sup>

In this study, a VWD mouse model with hepatic expression of mVWF was used. This model provided support for the concept of allele-specific VWF inhibition to correct for VWD phenotypes. Extra-hepatic siRNA delivery, including endothelial siRNA delivery, is more challenging. Fortunately, recent studies have shown promising results in downregulation of several endothelial genes by lipid or polymeric nanoparticles.<sup>30-32</sup> Future studies in which these nanoparticles are used to target VWF mutations in recently developed knock-in VWD mouse models are needed to prove that the approach of allele-specific VWF inhibition to correct VWD phenotypes is also promising in a model where mutant VWF is expressed in endothelial cells instead of the hepatocytes.<sup>33</sup>

Altogether we have shown that injection of an allele-specific siRNA that targets liver-expressed mVwf-p.Val1316Met in a heterozygous VWD type 2B mouse model, leads to correction of the VWD type 2B platelet phenotype. Decreased percentage of mutant mVWF in plasma after siRNA injection was noted, which coincided with an increase in platelet count and a decrease in platelet size and the mVWF activation factor. These results are promising for further studies on RNA-targeted therapies for VWD. It is, however, important to show that no off-target effects are induced. This should be proven by an experiment in which a mismatch negative control is taken along. Furthermore, future studies in endothelial knock-in models for VWD are needed to further elucidate the impact of allele-specific *Vwf* inhibition *in vivo*.

## References

1. Goodeve AC. The genetic basis of von Willebrand disease. *Blood Rev.* 2010;**24**(3):123-134.
2. De Ceunynck K, De Meyer SF, Vanhoorelbeke K. Unwinding the von Willebrand factor strings puzzle. *Blood.* 2013;**121**(2):270-277.
3. Leebeek FW, Eikenboom JC. Von Willebrand's Disease. *N Engl J Med.* 2016;**375**(21):2067-2080.
4. de Jong A, Eikenboom J. Von Willebrand disease mutation spectrum and associated mutation mechanisms. *Thromb Res.* 2017;**159**:65-75.
5. Hulstein JJ, de Groot PG, Silence K, Veyradier A, Fijnheer R, Lenting PJ. A novel nanobody that detects the gain-of-function phenotype of von Willebrand factor in ADAMTS13 deficiency and von Willebrand disease type 2B. *Blood.* 2005;**106**(9):3035-3042.
6. Blenner MA, Dong X, Springer TA. Structural basis of regulation of von Willebrand factor binding to glycoprotein Ib. *J Biol Chem.* 2014;**289**(9):5565-5579.
7. Casari C, Du V, Wu YP, et al. Accelerated uptake of VWF/platelet complexes in macrophages contributes to VWD type 2B-associated thrombocytopenia. *Blood.* 2013;**122**(16):2893-2902.
8. Casonato A, Gallinaro L, Cattini MG, et al. Reduced survival of type 2B von Willebrand factor, irrespective of large multimer representation or thrombocytopenia. *Haematologica.* 2010;**95**(8):1366-1372.
9. Federici AB, Mannucci PM, Castaman G, et al. Clinical and molecular predictors of thrombocytopenia and risk of bleeding in patients with von Willebrand disease type 2B: a cohort study of 67 patients. *Blood.* 2009;**113**(3):526-534.
10. Kruse-Jarres R, Johnsen JM. How to treat type 2B von Willebrand disease. *Blood.* 2018;**131**(12):1292-1300.
11. Casonato A, Sartori MT, Bertomoro A, Fede T, Vasoin F, Girolami A. Pregnancy-induced worsening of thrombocytopenia in a patient with type IIB von Willebrand's disease. *Blood Coagul Fibrinolysis.* 1991;**2**(1):33-40.
12. Hultin MB, Sussman II. Postoperative thrombocytopenia in type IIB von Willebrand disease. *Am J Hematol.* 1990;**33**(1):64-68.
13. Ranger A, Manning RA, Lyall H, Laffan MA, Millar CM. Pregnancy in type 2B VWD: a case series. *Haemophilia.* 2012;**18**(3):406-412.
14. de Jong A, Dirven RJ, Oud JA, Tio D, van Vlijmen BJM, Eikenboom J. Correction of a dominant-negative von Willebrand factor multimerization defect by small interfering RNA-mediated allele-specific inhibition of mutant von Willebrand factor. *J Thromb Haemost.* 2018;**16**(7):1357-1368.
15. Casari C, Pinotti M, Lancellotti S, et al. The dominant-negative von Willebrand factor gene deletion p.P1127\_C1948delinsR: molecular mechanism and modulation. *Blood.* 2010;**116**(24):5371-5376.
16. de Jong A, Dirven RJ, de Boer CM, et al. Allele-specific Inhibition of VWF p.Cys1190Tyr in Patient-Derived Endothelial Colony Forming Cells Corrects the von Willebrand Disease Type 2A Phenotype. *Res Pract Thromb Haemost.* 2019;**3**(Suppl S1 (OC56.2)):113.
17. Rayes J, Hollestelle MJ, Legendre P, et al. Mutation and ADAMTS13-dependent modulation of disease severity in a mouse model for von Willebrand disease type 2B. *Blood.* 2010;**115**(23):4870-4877.

18. Miller VM, Xia H, Marrs GL, et al. Allele-specific silencing of dominant disease genes. *Proc Natl Acad Sci U S A*. 2003;**100**(12):7195-7200.
19. Noguchi S, Ogawa M, Kawahara G, Malicdan MC, Nishino I. Allele-specific Gene Silencing of Mutant mRNA Restores Cellular Function in Ullrich Congenital Muscular Dystrophy Fibroblasts. *Mol Ther Nucleic Acids*. 2014;**3**:e171.
20. Ohnishi Y, Tamura Y, Yoshida M, Tokunaga K, Hohjoh H. Enhancement of allele discrimination by introduction of nucleotide mismatches into siRNA in allele-specific gene silencing by RNAi. *PLoS One*. 2008;**3**(5):e2248.
21. Golder M, Pruss CM, Hegadorn C, et al. Mutation-specific hemostatic variability in mice expressing common type 2B von Willebrand disease substitutions. *Blood*. 2010;**115**(23):4862-4869.
22. Legendre P, Navarrete AM, Rayes J, et al. Mutations in the A3 domain of von Willebrand factor inducing combined qualitative and quantitative defects in the protein. *Blood*. 2013;**121**(11):2135-2143.
23. Casari C, Paul DS, Susen S, et al. Protein kinase C signaling dysfunction in von Willebrand disease (p.V1316M) type 2B platelets. *Blood Adv*. 2018;**2**(12):1417-1428.
24. Eguchi A, De Mollerat Du Jeu X, Johnson CD, Nektaria A, Feldstein AE. Liver Bid suppression for treatment of fibrosis associated with non-alcoholic steatohepatitis. *J Hepatol*. 2016;**64**(3):699-707.
25. Odell TT, McDonald TP. Life span of mouse blood platelets. *Proc Soc Exp Biol Med*. 1961;**106**:107-108.
26. Gagnon KT, Corey DR. Guidelines for Experiments Using Antisense Oligonucleotides and Double-Stranded RNAs. *Nucleic Acid Ther*. 2019;**29**(3):116-122.
27. Heestermans M, de Jong A, van Tilburg S, et al. Use of “C9/11 Mismatch” Control siRNA Reveals Sequence-Related Off-Target Effect on Coagulation of an siRNA Targeting Mouse Coagulation Factor XII. *Nucleic Acid Ther*. 2019;**29**(4):218-223.
28. Singh SK, Nielsen P, Koshkin AA, Wengel J. LNA (locked nucleic acids): synthesis and high-affinity nucleic acid recognition. *Chem Commun*. 1998(4):455-456.
29. Malek-Adamian E, Fakhoury J, Arnold AE, Martinez-Montero S, Shoichet MS, Damha MJ. Effect of Sugar 2',4'-Modifications on Gene Silencing Activity of siRNA Duplexes. *Nucleic Acid Ther*. 2019;**29**(4):187-194.
30. Dahlman JE, Barnes C, Khan O, et al. In vivo endothelial siRNA delivery using polymeric nanoparticles with low molecular weight. *Nat Nanotechnol*. 2014;**9**(8):648-655.
31. Khan OF, Kowalski PS, Doloff JC, et al. Endothelial siRNA delivery in nonhuman primates using ionizable low-molecular weight polymeric nanoparticles. *Sci Adv*. 2018;**4**(6):eaar8409.
32. Fehring V, Schaeper U, Ahrens K, et al. Delivery of therapeutic siRNA to the lung endothelium via novel Lipoplex formulation DACC. *Mol Ther*. 2014;**22**(4):811-820.
33. Adam F, Casari C, Prevost N, et al. A genetically-engineered von Willebrand disease type 2B mouse model displays defects in hemostasis and inflammation. *Sci Rep*. 2016;**6**:26306.

